isomerization and aromatization constants were determined following the numerical methods used in [5] and [2], respectively. These values can be compared with those corresponding to the isomerization and aromatization of steranes, 91 and 200 kJ · mol^{-1}, respectively [3]. Other authors have found C-20 sterane isomerization energies of 145 [5], 131 [8], and 170 [8] kJ · mol^{-1}. In any case, the differences indicate that phyllocladane isomerization at C-16 may occur at the early stages of organic matter maturation (even earlier than those corresponding to sterane or hopane isomerization), whereas phyllocladane aromatization to retene may be characteristic of conditions involving important degrees of transformation, such as situations of high thermal stress.

Received May 21 and August 8, 1990

1. Rullkötter, J., et al.: Geochim. Cosmochim. Acta *45,* 1357 (1985)
2. Abbott, G. D., et al.: Org. Geochem. *6,* 31 (1984)
3. Mackenzie, A. S., McKenzie, D.: Geol. Mag. *120,* 417 (1983)
4. Mackenzie, A. S., et al.: Org. Geochem. *6,* 875 (1984)
5. Suzuki, S.: Geochim. Cosmochim. Acta *48,* 2273 (1984)
6. Lewan, M. D., et al.: ibid. *50,* 1977 (1986)
7. Alexander, R., et al.: Org. Geochem. *10,* 997 (1986)
8. Rullkötter, J., Marzi, R.: ibid. *13,* 639 (1988)
9. Alexander, G., et al.: Geochim. Cosmochim. Acta *51,* 2065 (1987)
10. Alexander, G., et al.: J. Chromatogr. *446,* 87 (1988)
11. Streibl, M., et al.: An. Quim. *68,* 879 (1972)
12. Noble, R. A., et al.: Geochim. Cosmochim. Acta *49,* 2141 (1985)

Naturwissenschaften 77, 536 – 538 (1990)

Controlled Biosynthesis of Greigite (Fe_3S_4) in Magnetotactic Bacteria

B. R. Heywood
School of Chemistry, University of Bath, Bath BA2 7AY, UK

D. A. Bazylinski
Department of Anaerobic Microbiology, Virginia Polytechnic Institute and State University, Blacksburg, VA 24061, USA

A. Garratt-Reed
Center for Materials Science and Engineering, Massachusetts Institute of Technology, Cambridge, MA 02139 USA

S. Mann
School of Chemistry, University of Bath, BATH BA 27 AY

R.B. Frankel
Department of Physics, California Polytechnic State University, San Luis Obispo, CA 93407, USA

Several species of aquatic bacteria have been identified which employ the earth's geomagnetic field to direct their motion towards suitable habitats. A common feature of these magnetotactic bacteria is the presence of discrete intracellular magnetic inclusions, *magnetosomes,* aligned in chains along the long axis of the organism. The size and orientation of these individual magnetic particles impart a permanent magnetic dipole moment which is responsible for the magnetotactic response. Until recently only crystals of the mixed-valence iron oxide, magnetite (Fe_3O_4), were identified in these bacteria. Now, however, magnetic and non magnetic iron sulfide minerals have been identified in multicellular magnetotactic bacteria collected from sulfidic environments [1, 2]. These studies showed the presence of discrete intracellular crystals but were in conflict with regard to their mineralogical identification, viz. pyrrhotite (FeS_{1+x}) [2] or greigite (Fe_3S_4) and pyrite (FeS_2) [1]. This discovery is of profound importance to the study of biomineralization, prokaryotic metabolism [3] and, possibly, the origin of life [4]. Here we report the presence of intracellular greigite crystals in two different types of rod-shaped single-celled magnetotactic bacteria collected from sulfide-rich sites. The greigite particles are often organized in chains, have narrow size distributions (50 – 90 nm), and adopt specific crystallographic habits (cubo-octahedral and rectangular prismatic) associated with particular cell types. The prismatic crystals are unusual since they do not conform to the symmetry relations of the greigite cubic lattice. Our results indicate that the biomineralization of greigite in magnetotactic bacteria is highly regulated and there are close similarities to the biosynthesis of bacterial magnetite (Fe_3O_4) [5, 6]. The formation of novel morphologies of biogenic greigite suggests that such crystals may provide a diagnostic marker in the characterization of sources of remanent magnetization in recent and ancient sediments [7].

Bacteria were collected from jars of sulfide-rich sediment and water sampled from salt-marsh pools at the Neponset River and Woods Hole, Massachusetts, and at Morro Bay, California. Permanent magnets were placed on the sampling jars with the south magnetic pole positioned just above the water-sediment interface and bacteria that accumulated near the pole were drawn up with a Pasteur pipette and examined by light microscopy. The bacteria collected in this manner included the multicellular magnetotactic

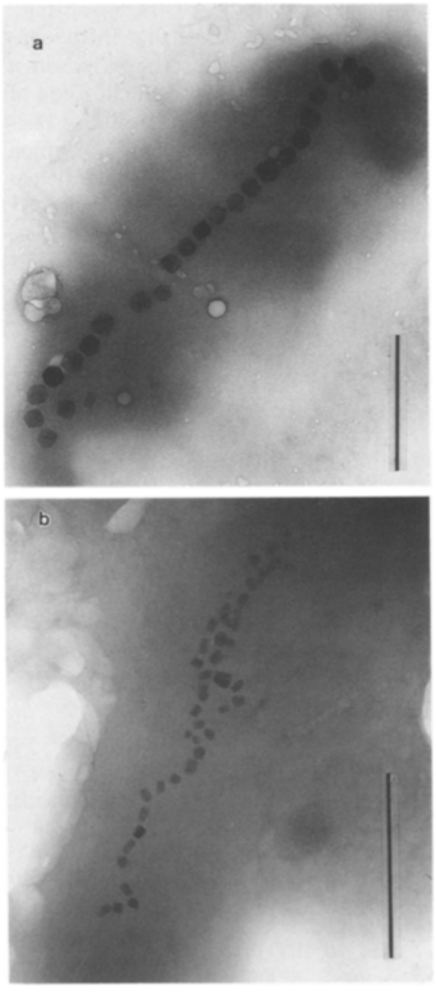

Fig. 1. Transmission electron micrographs ot two types of magnetotactic rod-shaped bacteria collected from sulfidic environments containing a) cubo-octahedral and b) rectangular prismatic iron sulfide inclusions. *Bar* 1 μm (a), 500 nm (b)

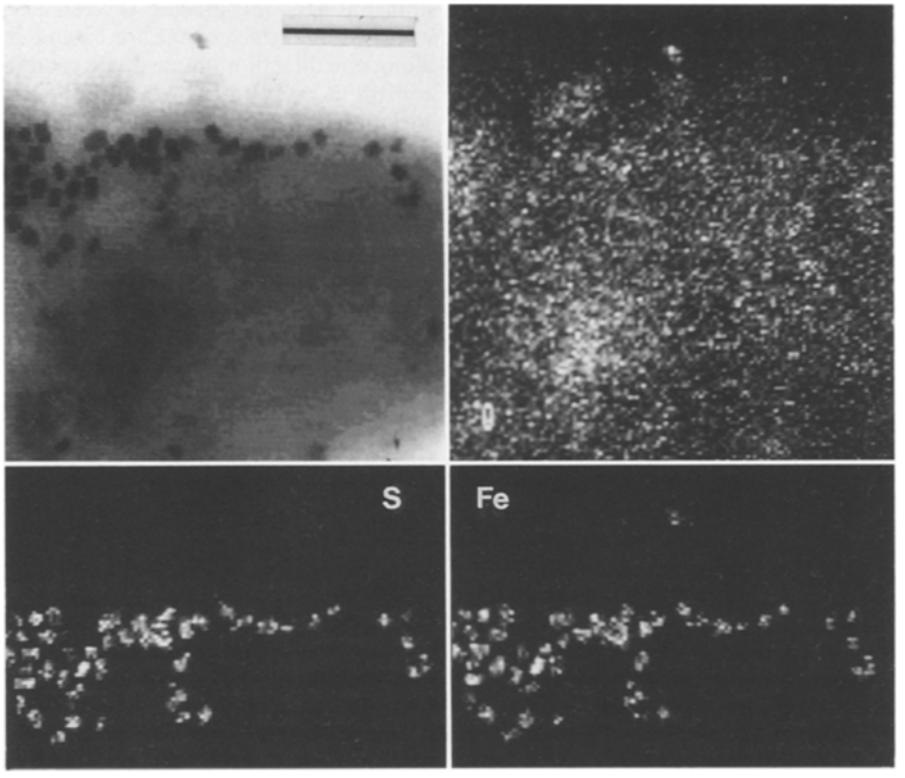

Fig. 2. Fe, S, and O elemental density maps for rectangular prismatic inclusions within a rod-shaped magnetotactic bacterium. The area analyzed is shown in the upper left-hand corner. Maps were produced by recording the respective x-ray intensities with the energy-dispersive x-ray detector at each position as the electron beam was slowly rastered across the area analyzed. Fe and S, but not O, correlate with particle position. Similar results were obtained for the cubo-octahedral particles in the smaller rod. *Bar* 500 nm

organism described previously [1, 2, 8, 9], as well as several morphological types of magnetotactic rod-shaped bacteria. The bacteria were subsequently deposited unstained on amorphous carbon films on nickel grids for electron microscopy. They were examined by scanning transmission electron microscopy (STEM), high-resolution transmission electron microscopy (HRTEM), and energy-dispersive X-ray analysis (EDXA), and electron diffraction. All crystallographic and elemental analyses were done on particles located within intact bacteria.

Transmission electron micrographs of two of the predominant types of magnetotactic rod are shown in Fig. 1. One type (Fig. 1b) was a large (ca. 3 × 2 μm) organism with chains and clusters of predominantly rectangular electron-dense particles. Individual cells contained, on average, 57 crystals of mean dimensions 69 × 50 nm with a variable aspect ratio (1.0 to 2.0). The crystals exhibited well-defined end faces but the sides were often irregular. A second cell type (Fig. 1a) was a smaller (ca. 2.5 × 1.3 μm) organism with a single chain of, on average, 26 well-defined cuboidal electron-dense particles of mean dimension, 67 nm. Elemental mapping of the particles by EDXA (Fig. 2) showed that both types of particles consisted of iron and sulfur but not oxygen.

Identification of the mineral phase in both cell types was made by indexing single-crystal electron diffraction patterns and lattice images of individual particles. This was necessary because the d-spacings of all the iron sulfides are similar, making identification from limited powder diffraction data alone unreliable. A single-crystal electron diffraction pattern from a rectangular particle in the larger rod-shaped bacterium is shown in Fig. 3a. The pattern corresponds to the <100> zone of greigite, (Fe_3S_4). Superposition of the pattern and corresponding image (see inset) indicates that the crystals are elongated along one of the *a* axes and the well-defined end faces and less regular side faces are of {100} form. These observations were confirmed by crystallographic analysis of greigite particles aligned along different directions e.g. [$\bar{1}$12], [2$\bar{1}\bar{5}$], and [110], and by lattice imaging (data not shown). Thus, the crystals have an idealized morphology based on a rectangular prism of six cubic {100} faces.

Single-crystal electron diffraction patterns from particles in the smaller rod-shaped bacteria were also indexed to greigite (Fig. 3b). Diffraction patterns corresponding to the [112], [21$\bar{3}$], and [01$\bar{1}$] zones of greigite were obtained. Analysis of the diffraction patterns and associated images, as well as lattice

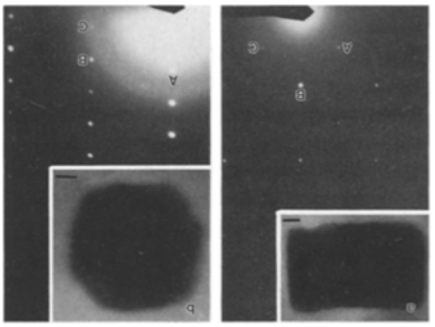

Fig. 3. Single-crystal greigite (Fe_3S_4) electron diffraction patterns recorded from iron sulfide inclusions and associated images (insets). a) Prismatic rectangular crystal viewed down the [001] zone. Reflection A, (220) (3.50 Å); reflection B, (400) (2.47 Å); reflection C, $(2\bar{2}0)$ (3.50 Å); angles: (220) $\wedge$(400) = 45°; (220) $\wedge$ $(2\bar{2}0)$ = 90°. b) Cubo-octahedral crystal viewed down the $[21\bar{3}]$ zone. Reflection A, (222) (2.86 Å); reflection B, $(4\bar{2}2)$ (2.017 Å); reflection C, $(3\bar{3}1)$ (2.28 Å); angles: (222 $\wedge 4\bar{2}2$ = 61.5°; 222 $\wedge 3\bar{3}1$ = 82.3°). *Scale bars* (insets) 10 nm

images of the crystals, indicated that the particles were cubo-octahedral in morphology with well-defined {111} faces and smaller truncated {100} faces. These results in conjunction with previous observations [1] suggest that the biomineralization of greigite may be a common occurrence in magnetotactic bacteria inhabiting sulfidic environments. Interestingly, the rod-shaped bacteria appear to maintain greater control over mineralization compared with a previously described multicellular organism. The latter produces crystals of both greigite and pyrite (FeS_2) [1] and the morphologies are not well-defined [1,2]. By contrast, the rod-shaped bacteria specifically mineralize greigite and regulate the crystal habit. While the deposition of cubo-octahedral crystals may reflect an equilibrium form involving minimal biological intervention, the formation of elongated cubic crystals indicates that the biosynthetic mechanism involves disruption of the symmetry relationships in the isometric lattice of greigite. A similar effect has also been observed with bacterial magnetites [5]. One possibility is that the greigite crystals develop within vesicles that are extended along one direction, imparting a spatial constraint in crystal growth. But the association of a preferred crystallographic axis (<100>) with the direction of elongation suggests that the greigite crystals are oriented during nucleation, indicating that mineralization is also regulated at the molecular level.

Assuming that the 67-nm particles in the smaller rod are single-magnetic-domains, it is possible to calculate the average permanent magnetic dipole per cell [10]. A greigite density of 4.1 g/cm^3 from the crystallographic data (space group, *Fd3m*, a = 9.88 Å, 8 formula units per unit cell) and a measured saturation magnetization of 30 emu/g [11] yields a permanent magnetic dipole moment per particle, $m = 3.65 \times 10^{-14}$ emu. For particles arranged in a chain, the total moment is the sum of the individual particle moments [10]. Thus, the total moment of a cell with a chain of 26 particles, $M = 9.5 \times 10^{-13}$ emu. In the geomagnetic field, B_G = 0.5 Gauss, the magnetic energy, $M \times B_G \approx 4 \times 10^{-13}$ erg, which is more than ten times thermal energy at 300 K. Thus, the chain of greigite particles has a large enough permanent magnetic dipole moment so that the migration speed of the cell along geomagnetic field lines would be more than 80 % of its forward speed [10]. If some particles in the chain were nonmagnetic pyrite, as they are in the case of the multicellular organism [1], the migration efficiency would be correspondingly reduced. The average permanent magnetic dipole moment of the larger rod-shaped cells is not so easily calculated because the relative orientations of the individual particle moments in the clusters are not known. The fact that the larger rods contain more particles on average could reflect the magnetically less efficient arrangement of the elongated particles compared to the ordered chains in the smaller rod-shaped cells.

The foregoing analysis suggests that the rod-shaped bacteria specifically mineralize greigite, not pyrite, in connection with magnetotaxis. This specificity argues against the view that intracellular greigite transforms to pyrite on a time scale comparable to the lifetime of the cell [1]. Thus, the multicellular bacterium recently described [1], which contains greigite and pyrite, may be capable of simultaneously and separately mineralizing the two iron sulfides. Since pyrite does not contribute to the magnetotactic response, its role may be related to the maintenance of homeostasis of iron and/or sulfide [3], or to other metabolic processes in the cells.

We thank R.P. Blakemore for discussions. R.B.F. was supported by the US National Science Foundation and B.R.H. by BP International Ltd.

Received August 13, 1990

1. Mann, S., Sparks, N.H.C., Frankel, R.B., Bazylinski, D.A., Jannasch, H.W.: Nature *343,* 258 (1990)
2. Farina, M., Motta de Esquivel, D., Lins de Barros, H.G.P.: ibid. *343,* 256 (1990)
3. Williams, R.J.P.: ibid. *343,* 213 (1990)
4. Wächterhäuser, G.: Syst. Appl. Microbiol. *10,* 207 (1988)
5. Mann, S., Frankel, R.B., in: Biomineralization: Chemical and Biochemical Perspectives, p. 389 (eds. Mann, S., Webb, J., Williams, R.J.P.). Weinheim: VCH 1989
6. Blakemore, R.P.: Ann. Rev. Microbiol. *36,* 217 (1982)
7. Demitrack, A., in: Magnetite Biomineralization and Magnetoreception in Organisms, p. 625 (eds. Kirchvink, J.L., Jones, D.S., Macfadden, B.F.). New York: Plenum 1985
8. Rodgers, F.G., Blakemore, R.P., Blakemore, N.A., Frankel, R.B., Bazylinski, D.A., Maratea, D., Rodgers, C.: Arch. Microbiol. *154,* 18 (1990)
9. Farina, M., Lins de Barros, H.C.P., Esquivel, D.M.S., Danon, J.: Biol. Cell *48,* 85 (1983)
10. Frankel, R.B.: Ann. Rev. Biophys. Bioeng. *13,* 85 (1984)
11. Spender, R.M., Coey, J.M.D., Morrish, A.H.: Can. J. Phys. *50,* 2313 (1972)

